JPEDAV (2015) 36:375–380
DOI: 10.1007/s11669-015-0394-2
1547-7037 ©ASM International

Experimental Study of the Phase Relations in the Zn-Co-Sb Ternary System at 600 °C

Zhongxi Zhu, Meiliang Chen, Wei Zhu, and Fucheng Yin

(Submitted March 20, 2015; in revised form May 2, 2015; published online June 30, 2015)

The 600 °C isothermal section of the Zn-Co-Sb ternary system has been determined experimentally by means of scanning electron microscopy coupled with energy-dispersive spectrometry and x-ray diffraction. Nine three-phase regions could be confirmed in the isothermal section at 600 °C. Moreover, a new ternary compound named CoSbZn was positively identified for the first time in this study, containing 25.8 to 39.0 at.% Co, 28.9 to 36.4 at.% Zn and 31.4 to 38.0 at.% Sb. The experimental results indicated that the maximum solubility of Co in the L phase was less than 2.4 at.%.

Keywords CoSbZn, phase diagram, SEM, Zn-Co-Sb system

1. Introduction

The hot-dip zinc coatings have been widely used for protection of steel against corrosion.[1] Adding alloying elements such as Ni, Bi, V and Ti[2–6] into zinc bath is an effective method to obtain high-quality coatings. Recently, Li et al.[7] and Zhao et al.[8] have investigated the effect of Co in zinc bath on the microstructures and growth dynamics of the hot-dip galvanizing coating. Their results show that the addition of Co into zinc bath can improve the quality of hot-dip galvanizing coating.

In the primitive hot-dip galvanizing technology, Pb was added to the bath to enhance the fluidity of molten zinc and promote the spangles growth on the coating surface. Galvanizing with Pb-containing alloys damages the environment and is bad for humans. It was forbidden in some countries.[9–11] Recently, it was found that Sb has a function similar to Pb and is better than the addition of Pb,[12] because it has a very low segregation coefficient and a correspondingly high solute concentration in the melt at the interface.[13] Besides, Sb exists in the coating in the form of Sb_2Zn_3 compound which improves the intergranular corrosion resistance of the coating. At present, the optimum addition of Sb is not more than 0.01 at.%.[14]

In view of significant influence of Co and Sb additions to Fe-Zn baths, it is important to have some knowledge of the phase diagram on the Zn-Fe-Co-Sb quaternary system. This system has four ternary systems, i.e. Zn-Fe-Co,[15] Zn-Fe-Sb,[16] Fe-Co-Sb[17] and Zn-Co-Sb. Except Zn-Co-Sb ternary system, the other ternary systems have been experimentally investigated. In order to obtain reliable phase relations and enough data for thermodynamic calculation of Zn-Co-Sb ternary system, the 600 °C isothermal section has been determined experimentally in the present work.

Zhongxi Zhu, Meiliang Chen, and **Fucheng Yin,** Key Laboratory of Materials Design and Preparation Technology of Hunan Province, Xiangtan, Hunan, People's Republic of China and School of Mechanical Engineering, Xiangtan University, Xiangtan 411105, Hunan, People's Republic of China; and **Wei Zhu,** School of Mathematics and Computational Science, Xiangtan University, Xiangtan 411105, Hunan, People's Republic of China. Contact e-mail: Zzx552@xtu.edu.cn.

2. Literature Review

Zn-Co-Sb ternary system consists of three binary phase diagrams, Co-Zn, Co-Sb and Zn-Sb. Okamoto[18] and Vassilev et al.[19] have been summarized many experimental data on the Co-Zn phase diagram, through the newest phase diagram,we can see six intermetallic compounds in the Co-Zn system, viz., β_1-CoZn, β-CoZn, γ-Co_5Zn_{21}, γ_1-$CoZn_{7.8}$, γ_2-$CoZn_{13}$ and δ-Co_2Zn_{15}. However, the β-CoZn, γ_2-$CoZn_{13}$ and δ-Co_2Zn_{15} don't exist in 600 °C. The most recent experiment phase diagram of Co-Sb was updated by Okamoto[20] based on Hanninger.[21] Kjekshus et al.[22] investigated the thermal stability of $CoSb_2$ by XRD and DTA and determined the polymorphic transformation from γ-$CoSb_2$ to γ′-$CoSb_2$ at 650 K. There are four intermetallic compounds in the Co-Sb system, viz. β-CoSb, γ-$CoSb_2$, γ′-$CoSb_2$ and δ-$CoSb_3$. The phase diagram of the Zn-Sb system has been studied extensively by many authors.[23–26] Recently the Sb-Zn phase diagram was re-investigated by Izard et al.[25] with high-temperature x-ray diffraction technique. They found that high-temperature polymorphic forms of Sb_3Zn_4 and Sb_2Zn_3 exist. The crystallographic parameters of the binary compounds involved in the present work at 600 °C are listed in Table 1.

3. Experimental Methods

The phase relationships of the Zn-Co-Sb ternary system are deduced by studying nine alloy samples. The nominal

compositions of these alloys are listed in Table 2. The purity of raw materials, i.e., Sb and Co powders and Zn chips was 99.99 wt.%. The mixture of the raw materials on the required proportion, with a total weight of 5 g, was sealed in an evacuated quartz tube. Each mixture was heated slowly to a temperature above its estimated liquids temperature and kept long enough to obtain uniformly, followed by quenching in water using a bottom-quenching technique[27] to minimize Zn loss and reduce sample porosity. The quenched samples were then resealed and annealed at 600 °C for 30 days, to ensure the establishment of an equilibrium state. The treatment was completed with rapid water quenching to preserve the equilibrium state at the annealing temperature.

Sections of the specimens were prepared in the conventional way for metallographic examinations. The 4% nital etching solution was used for revealing the microstructural details and a conventional optical microscope was used for the preliminary examination of all specimens. Detailed metallographic examinations and compositional analyses of various phases in the samples were performed using a JSM-6360LV scanning electron microscope (SEM) coupled with OXFORD INCA energy-dispersive spectrometric (EDS) under backscattered electron image (BSE) mode. The compositions reported in this study are the averages of at least five measurements. The constituent phases in the alloys were further determined by analyzing the x-ray diffraction

Table 1 Crystallographic data of the binary compounds in the Zn-Co-Sb ternary system at 600 °C

Compound	Space group	Structure type	Lattice parameters, Å			Refs
			a	*b*	*c*	
β_1-CoZn	$P4_132$	βMn	6.3450	…	…	[28]
γ-Co_5Zn_{21}	*I*-43 m	Cu_5Zn_8	8.9270	…	…	[29]
γ_1-$CoZn_{7.8}$	*F2/m*	γ-brass related	9.0300	4.3380, β = 89.9°	12.5110	[30]
CoSb	$P6_3/mmc$	NiAs	3.8900	…	5.1870	[31]
$CoSb_2$	$P2_1/c$	$CoSb_2$	6.5200	6.3800, β = 118.2°	6.5500	[32]
$CoSb_3$	*Im-3*	$CoAs_3$	9.0385	…	…	[33]

Table 2 Alloys and phase compositions in the Zn-Co-Sb ternary system at 600 °C (at.%)

Alloys	Designed composition	Phase	Co	Zn	Sb
B1	$Co_5Zn_5Sb_{90}$	α-Sb	0.2	0.2	99.6
		$CoSb_3$	24.2	0.3	75.5
		L	0.4	9.1	90.5
B2	$Co_{20}Zn_{18}Sb_{62}$	$CoSb_2$	33.3	1.0	65.7
		$CoSb_3$	24.0	0.9	75.1
		L	1.1	51.8	47.1
B3	$Co_{26}Zn_{28}Sb_{46}$	$CoSb_2$	33.7	0.7	65.6
		CoSbZn	29.7	32.3	38.0
		L	1.4	54.1	44.5
B4	$Co_{42}Zn_{10}Sb_{48}$	$CoSb_2$	34.4	0.5	65.1
		CoSb	48.7	0.7	50.6
		CoSbZn	33.7	29.9	36.4
B5	$Co_{42}Zn_{29}Sb_{29}$	CoSb	48.4	2.3	49.3
		CoSbZn	39.0	28.9	32.1
		β_1	45.6	53.4	1.0
B6	$Co_{38}Zn_{42}Sb_{20}$	CoSbZn	36.4	32.2	31.4
		β_1	45.7	54.2	0.1
		γ	26.3	73.2	0.5
B7	$Co_{19}Zn_{74}Sb_7$	CoSbZn	25.8	36.4	37.8
		γ	18.7	80.0	1.3
		L	2.4	60.1	37.5
B8	$Co_{10}Zn_{80}Sb_{10}$	γ	16.3	82.8	0.9
		γ_1	11.3	88.5	0.2
		L	2.3	64.0	33.7
B9	$Co_{55}Zn_{38}Sb_7$	CoSb	49.2	1.8	49.0
		β_1	49.6	50.2	0.2
		α-Co	90.1	9.4	0.5

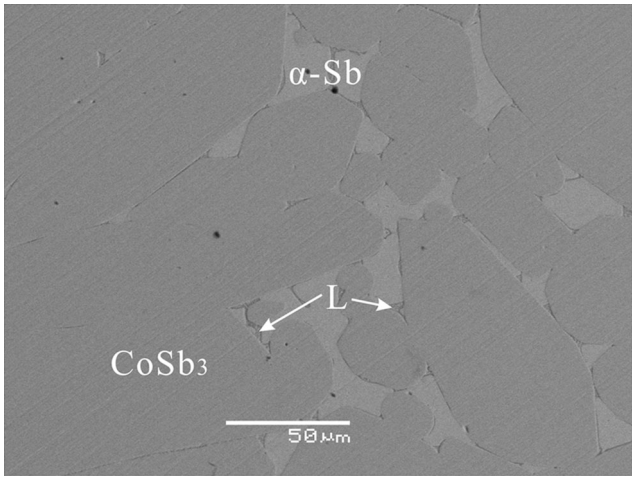

Fig. 1 The microstructure of Alloy B1 ($Co_5Zn_5Sb_{90}$): (α-Sb), $CoSb_3$ and L

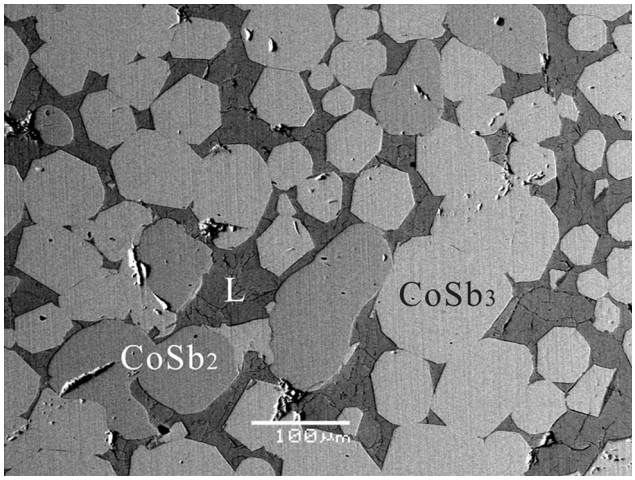

Fig. 2 The microstructure of Alloy B2 ($Co_{20}Zn_{18}Sb_{62}$): Three-phase region of $CoSb_3$, $CoSb_2$ and L

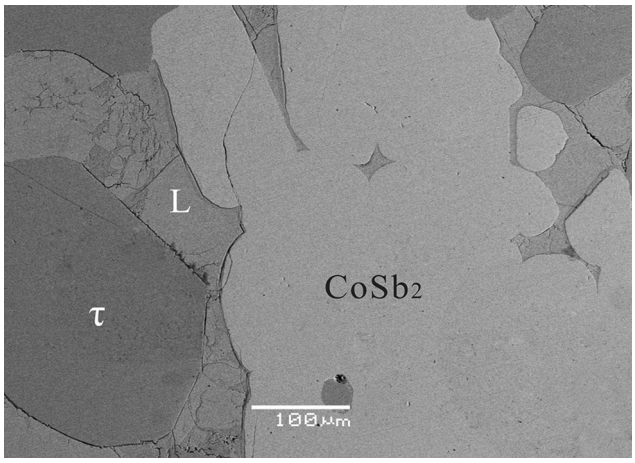

Fig. 3 BSE micrograph of $CoSb_2$, CoSbZn and L in alloy B3 ($Co_{26}Zn_{28}Sb_{46}$)

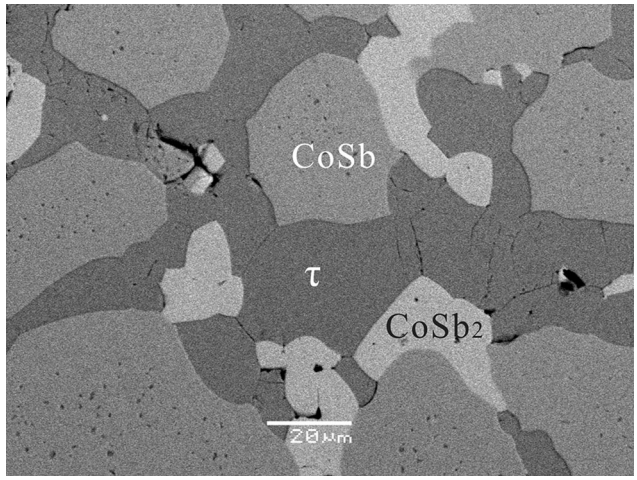

Fig. 4 The BSE micrograph of alloy B4 ($Co_{42}Zn_{10}Sb_{48}$) shows the three phases $CoSb_2$, CoSb and CoSnZn

patterns generated by a D/max-rA x-ray diffractometer, operating at 40 kV and 100 mA with Cu Kα radiation.

4. Results and Discussion

The design compositions of the alloys are listed in Table 2 (column 2). The composition of the phases identified as determined by the EDS technique are summarized in the table (column 4, 5 and 6). The compositions are the averages of at least five measurements. These phases were also confirmed by analyzing their x-ray diffraction patterns.

The microstructure of alloy B1 ($Co_5Zn_5Sb_{90}$) is shown in Fig. 1, in which α-Sb, $CoSb_3$ and liquid phase (marked as L in the present work) coexist.

The microstructure of alloy B2 ($Co_{20}Zn_{18}Sb_{62}$) is shown in Fig. 2. SEM-EDS analyses indicated that the gray block is $CoSb_2$ phase, the light gray block is $CoSb_3$ phase and the matrix phase is L.

An important discovery of this study is the new ternary compound, denoted CoSbZn, containing 25.8 to 39.0 at.% Co, 28.9 to 36.4 at.% Zn and 31.4 to 38.0 at.% Sb. Alloys B3-B7 are designed around CoSbZn. The micrograph of alloy B3 ($Co_{26}Zn_{28}Sb_{46}$) is shown in Fig. 3 which reveals that the alloy corresponds to $CoSb_2$ + L + CoSbZn three-phase equilibrate state.

Figure 4 and 5(c) show the microstructure and XRD pattern of alloy B4 ($Co_{42}Zn_{10}Sb_{48}$), and the difference in the relief of the three phases is remarkable. The white block $CoSb_2$ phase and the gray block CoSb phase coexist with CoSbZn phase.

The microstructure of alloy B5 ($Co_{42}Zn_{29}Sb_{29}$) which located in the (CoSb + β_1 + CoSbZn) three-phase region is given in Fig. 5a, and the XRD pattern is shown in Fig. 5(c). The solubility of Zn in the gray CoSb phase is 2.3 at.%. Alloy B6 ($Co_{38}Zn_{42}Sb_{20}$) contains β_1, γ and CoSbZn phase, and the microstructure and XRD pattern are shown in Fig. 5(b) and (c).

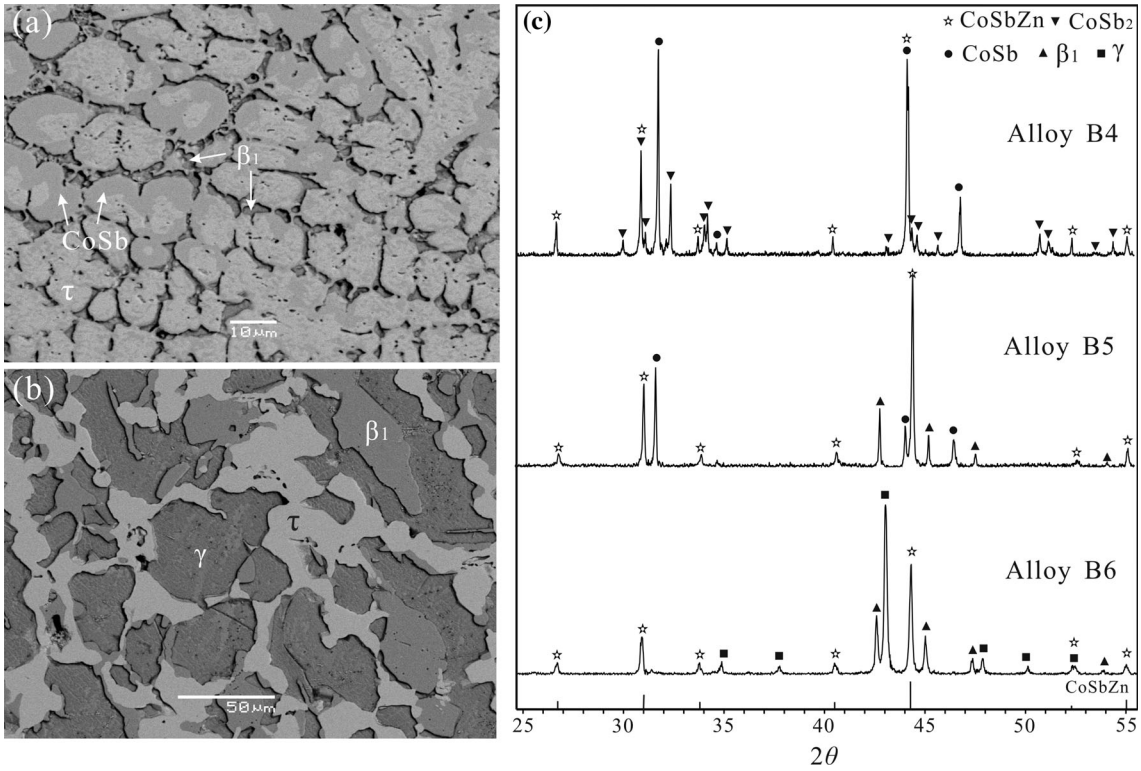

Fig. 5 (a) BSE micrograph of alloy B5 ($Co_{42}Zn_{29}Sb_{29}$). (b) BSE micrograph of alloy B6 ($Co_{38}Zn_{42}Sb_{20}$). (c) X-ray diffraction pattern of alloys B4, B5 and B6

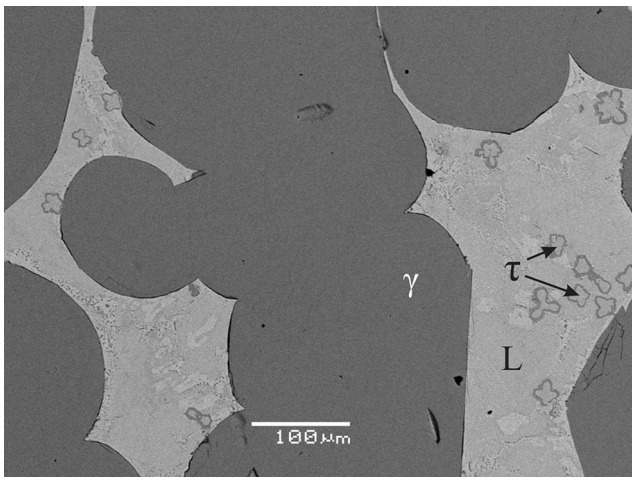

Fig. 6 The microstructure of Alloy B7 ($Co_{19}Zn_{74}Zn_7$) consists of three phases; γ, L and CoSbZn

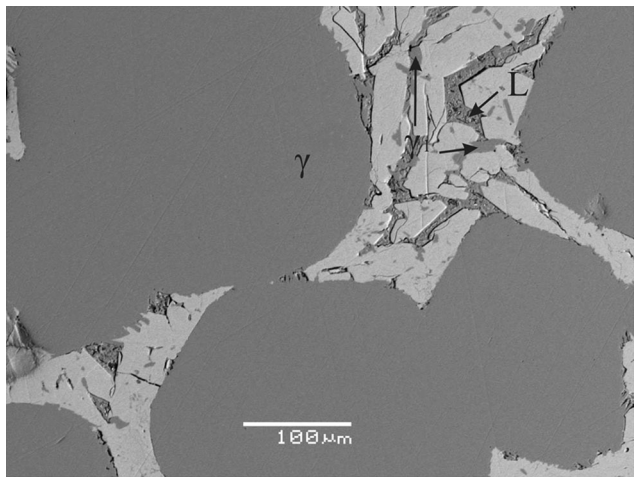

Fig. 7 BSE micrograph of the alloy B8 ($Co_{10}Zn_{80}Sb_{10}$)

Figure 6 shows the microstructure of alloy B7 ($Co_{19}Zn_{74}Sb_7$), and the relief of the three phases is remarkable. The white L phase and the butterfly shaped CoSbZn coexist with the matrix of the γ phase. The Sb-Zn compound (white blocks in the L phase) precipitated during water quenching. The L phase contains 2.4 at.% Co, and the γ phase contains 1.3 at.% Sb. According to the above result, the CoSbZn phase is in equilibrium with $CoSb_2$, CoSb, γ, γ_1 and L.

Alloy B8 (Co10Zn80Sb10) contains three phases: γ, γ_1 and L. As can be seen in Fig. 7, they can be well distinguished by their microstructure. The γ phase is dark gray matrix phase and γ_1 is between crystals of the Sb-Zn compound. The Sb-Zn compound (white blocks in the L phase) precipitated during the water quenching.

Figure 8 is the microstructure of Alloy B9 ($Co_{55}Zn_{38}Sb_7$). The white block CoSb phase and black block Co phase were evenly distributed in the matrix β_1 phase.

Based on the x-ray diffraction and SEM-EDS results in this work, along with the information of the binary systems in the literature, the 600 °C isothermal sections of Zn-Co-Sb ternary system is constructed, as shown in Fig. 9.

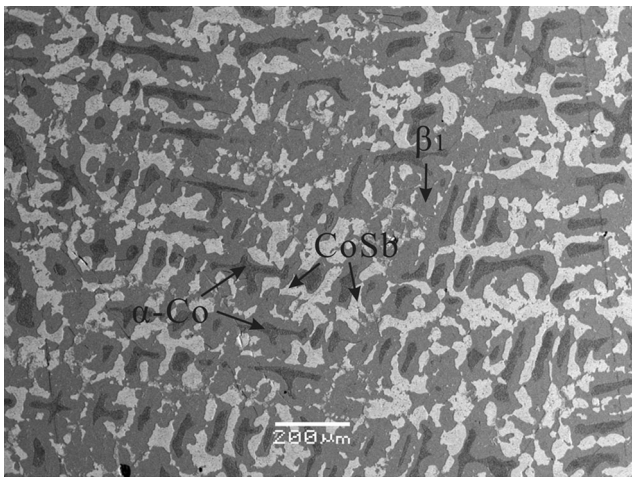

Fig. 8 The microstructure of Alloy B9 ($Co_{55}Zn_{38}Sb_7$) consists of three phases; (α-Co), CoSb and β_1

5. Conclusions

Based on SEM-EDS analyses and x-ray diffraction results, the 600 °C isothermal section of the Zn-Co-Sb ternary system is determined in the present work. The main conclusions are listed below:

1. Nine three-phase regions have been determined experimentally in the isothermal section at 600 °C.
2. The ternary compound CoSbZn contains 25.8 to 39.0 at.% Co, 28.9 to 36.4 at.% Zn and 31.4 to 38.0 at.% Sb at 600 °C.
3. The CoSbZn phase is in equilibrium with CoSb, $CoSb_2$, β_1-CoZn, γ-Co_5Zn_{21} and L at 600 °C.
4. The maximum solubility of Co in L phase is 2.4 at.%. The maximum solubility of Zn in CoSb is 2.3 at.%.

Acknowledgment

The investigation is supported by National Natural Science Foundation of China (Nos. 51371156 and 51471141).

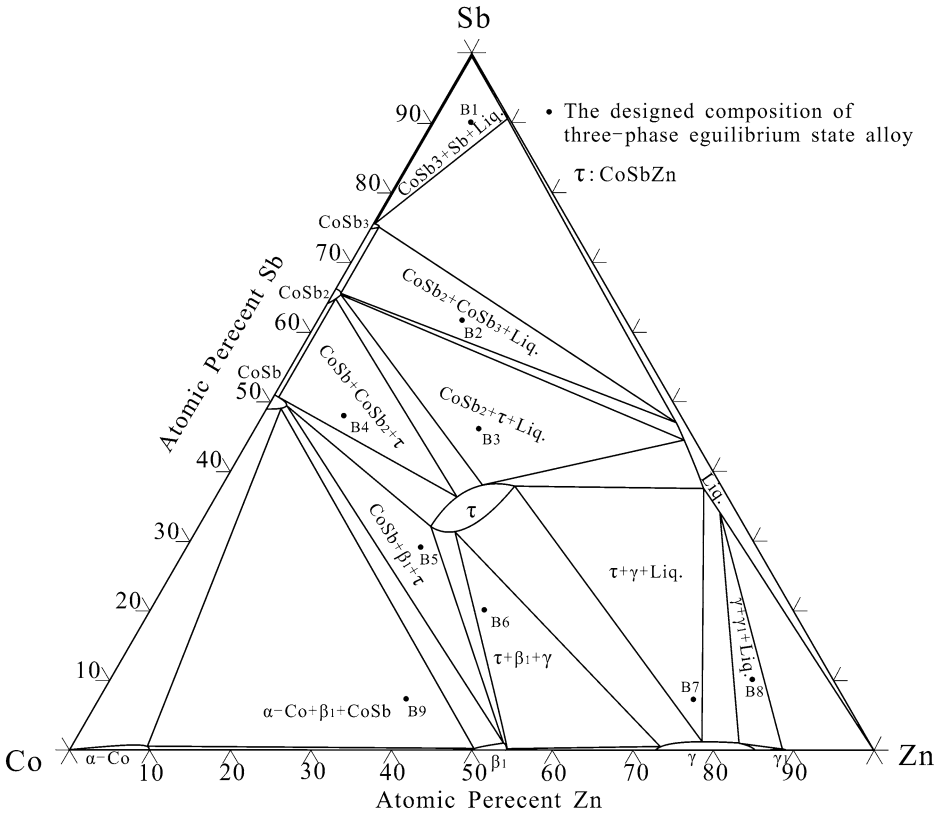

Fig. 9 The isothermal section of the Zn-Co-Sb ternary system at 600 °C

References

1. W. Bleck and D. Beste, Hot-Dip Coating, *Mod. Surf. Technol.*, 2006, **15**, p 221-237
2. R. Fratesi, N. Ruffini, M. Malavolta, and T. Bellezze, Contemporary Use of Ni and Bi in Hot-Dip Galvanizing, *Surf. Coat. Technol.*, 2002, **157**, p 34-39
3. A.R.P. Ghuman and J.L. Goldstein, Reaction Mechanisms for the Coatings Formed During the Hot Dipping of Iron in 0 to 10 Pct A1-Zn Baths at 450° to 700 °C, *Metall. Trans.*, 1971, **2**, p 2903-2914
4. C. Xu, F.C. Yin, M.X. Zhao, Y.X. Liu, and X.P. Su, Phase Equilibria of the Zn-Bi-Ni System at 600 and 750 °C, *J. Alloys Compd.*, 2010, **506**(1), p 125-130
5. Z. Li, Y.J. Gong, F.C. Yin, X.M. Wang, and M.X. Zhao, The 600 and 700 °C Isothermal Section of the Zn-Fe-Bi Ternary Phase, *J. Phase Equilib.*, 2011, **53**(3), p 528-546
6. X.H. Tang, F.C. Yin, X.M. Wang, J.H. Wang, and X.P. Su, The 450 °C Isothermal Section of the Zn-Fe-Ti System, *J. Phase Equilib.*, 2007, **28**, p 355-361
7. F.G. Li, F.C. Yin, X.P. Su, and Z. Li, Effect of Co on Microstructures and Growth Kinetics of Galvanizing Coating on Si Containing Steel, *Chin. J. Nonferrous Met.*, 2010, **20**, p 86-91
8. M.X. Zhao, F.C. Yin, Z. Li, Z.H. Long, and X.M. Wang, 450 °C Isothermal Section of the Zn-Fe-Co-Si Quaternary System at the Zinc-Rich Corner, *Int. J. Mater. Res.*, 2013, **104**, p 35-45
9. S. Chang and J.C. Shin, Effect of the Zinc Bath Composition on Hot Dip Galvanized and Galvannealed Steel Sheet, *Galvatech 95th Conference Proceedings,* Chicago, 1995, p 783-786
10. N. Pistofidis, G. Vourlias, S. Konidaris, E. Pavlidou, A. Stergiou, and G. Stergioudis, Microstructure of Zinc Hot-Dip Galvanized Coatings Used for Corrosion Protection, *Mater. Lett.*, 2006, **60**, p 786-789
11. N. Irving Sax, *Dangerous Properties of Industrial Materials*, VNR, New York, 1979
12. M. Dutta, A. Mukhopadhyay, and S. Chakrabarti, Effect of Galvanising Parameters on Spangle Size Investigated by DataMining Technique, *ISIJ Int.*, 2004, **44**(1), p 129-138
13. J. Strutzenberger and J. Faderl, Solidification, Spangle Formation of Hot-Dip—Galvanized Zinc Coatings, *Metall. Mater. Trans A*, 1998, **29**(2), p 631-646
14. Y.K. Shindou and M. Kabeya, Zn-Al Hot-Dip Galvanized Steel Sheet Having Improved Resistance Against Secular Peeling of Coating, U.S. Patent 4812371, 1989
15. V. Raghavan, Co-Fe-Zn (Cobalt-Iron-Zinc), *J. Phase Equilib.*, 2003, **24**, p 551-553
16. Z.X. Zhu, X.P. Su, and J.H. Wang, Experimental Investigation and Thermodynamic Calculation of the Zn-Fe-Sb System, *CALPHAD*, 2010, **34**, p 98-104
17. W. Geller, The Iron-Cobalt-Antimony System, *Arch. Eisenhüttenwes*, 1939, **13**, p 263-266
18. H. Okamoto, Co-Zn (Cobalt-Zinc), *J. Phase Equilib.*, 2007, **28**(3), p 315
19. G.P. Vassiley and M. Jiang, Thermodynamic Optimization of the Co-Zn System, *J. Phase Equilib.*, 2004, **25**(3), p 259-268
20. H. Okamoto, Co-Sb (Cobalt-Antimony), *J. Phase Equilib.*, 1991, **12**(2), p 244-245
21. G. Hanninger, H. Ipser, P. Terzieff, and K.L. Komarek, The Co-Sb Phase Diagram and Some Properties of NiAs-Type-Co1 ± xSb, *J. Less-Common Met.*, 1990, **166**, p 103-114
22. A. Kjekshus and T. Rakke, High Temperature Studies of Marcasite and Arsenopyrite Type Compounds, *Acta Chem. Scand. A*, 1977, **31**, p 517-529
23. X. Liu, C. Wang, I. Ohnuma, R. Kainuma, and K. Ishida, Thermodynamic Assessment of the Phase Diagrams of the Cu-Sb and Sb-Zn Systems, *J. Phase Equilib.*, 2000, **21**(5), p 432-442
24. J.-B. Li, M.-C. Record, and J.-C. Tedenac, A Thermodynamic Assessment of the Sb-Zn System, *J. Alloys Compd.*, 2007, **438**(1–2), p 171-177
25. V. Izard, M.C. Record, J. Haines, and J.C. Tedenac, Sb_3Zn_4, A Promising New Thermoelectric Material: Elaboration and Characterization, *Mat. Res. Soc. Symp. Proc.*, 2002, **691**, p 313
26. T. Takei, *Tohoku Imperial University-Science Reports.,* 1927, **16**(8), p 103-105
27. N.-Y. Tang, X. Su, and J.M. Toguri, Experiment Study and Thermodynamic Assessment of the Zn-Fe-Ni System, *Calphad*, 2001, **25**, p 267
28. F. Lihl and E. Weisberg, Phase Boundaries in the System Co-Zn, *Z. Metallkd.*, 1955, **46**, p 579-581
29. W. Ekman, X-Ray Studies of the Cobalt-Zinc Gamma-Phase, *Z. Phys. Chem. B*, 1931, **12**, p 57-78
30. H. Lind, M. Bostrom, V. Petricekc, and S. Lidina, Structure of d1-CoZn7.8, An Example of A Phason Pinning-Unpinning Transformation?, *Acta. Crystallogr. B*, 2003, **59**, p 720-729
31. A. Kjekshus and K.P. Walseth, On the Properties of the $Cr_{1+x}Sb$, $Fe_{1+x}Sb$, $Co_{1+x}Sb$, $Ni_{1+x}Sb$, $Pd_{1+x}Sb$, and $Pt_{1+x}Sb$ Phases, *Acta Chem. Scand.*, 1969, **23**, p 2621-2630
32. K. Ishida and T. Nishizawa, The Co-Sb (Cobalt-Antimony) System, *J. Phase Equilib.*, 1990, **11**(3), p 243-248
33. T. Schmidt, G. Kliche, and H.D. Lutz, Structure Refinement of Skutterudite-Type Cobalt Triantimonide, $CoSb_3$, *Acta Crystallogr. Sect. C*, 1987, **43C**, p 1678-1679